# Read/Interrogation Enhancement of Chipless RFIDs Using Machine Learning Techniques

Soyeon Jeong , *Student Member, IEEE*, Jimmy G. D. Hester , *Student Member, IEEE*, Wenjing Su , *Member, IEEE*, and Manos M. Tentzeris , *Fellow, IEEE*

*Abstract*—This letter describes the implementation of a machine learning (ML) classification strategy for read/interrogation enhancement in chipless radio frequency identification (RFID) applications. A novel ML-based approach for classification and of detection tag identifications (IDs) has been presented, which can perform effective transponder readings for a wide variety of ranges and contexts, while providing tag-ID detection accuracy of up to 99.3%. Four tags encoding the four 2 bit IDs were inkjet-printed onto flexible low-cost polyethylene terephtalate substrates and interrogated without crosstalk or clutter interference de-embedding at ranges up to 50 cm, with different orientations and with and without the presence of scattering objects in the vicinity of the tags and reader. A support vector machine algorithm was then trained using 816 measurements, and its accuracy was tested and characterized as a function of the included training data. Finally, the excellent performance of the approach, displaying reading accuracies ranging from 89.6% to 99.3%, is reported. This effort sets a precedent, opening the door to a rich and wide area of research for the implementation of ML methods for the enhancement of chipless RFID applications.

*Index Terms*—Chipless radio frequency identification (RFID) system, inkjet-printed tags, Internet of things, machine learning (ML), support vector machine (SVM).

## I. INTRODUCTION

RADIO frequency identification (RFID) technology is a rapidly growing wireless technology used to track and identify objects using HF, very high frequency (VHF), and RF waves automatically. With the RFID reader, which is known as an interrogator, the RFID transponder, the data are encoded and transmitted by an RFID tag [1]. Printable chipless RFIDs are a particularly appealing solution in contexts where cost is one of the most relevant constraints, as reported in [2]. However, these are very limited in reading range (a few meters) as a consequence of their linear operation and their sensitivity to interference. Crosstalk between reader antennas and environmental clutter interference can, however, be de-embedded, but this approach cannot account for large contextual changes in the vicinity of the tag and reader. Also, the most commonly used tag detection techniques require the knowledge of signal-processing methods or the careful and manual tuning of parameters, including background subtraction, time gating, continuous wavelet transform, and match filtering, in the reader side to process backscattered signal and extract the tag's data. Here, the authors propose an alternative approach that takes advantage of the immense pattern classification capabilities of modern machine learning (ML) techniques. For pattern classification, the support vector machine (SVM) classification is used not only to make the reliable prediction, but also to reduce redundant information. Especially, this technique provides an excellent performance when dealing with high-dimensional input data taking advantage of the fact that due to its generalization properties, the performance of the SVM does not depend on the dimensions of the space. The SVMs also obtained results comparable with those obtained by other classification methods utilizing the ML strategy. Using these, it is possible to forego the aforementioned calibration approaches while retaining accurate reading capabilities. In order to demonstrate this, a set of 2 bit chipless RFID tags with two T-shaped resonators encoding two distinct bits were first printed, and their properties were described and measured. Then, an ML approach is devised, presented, and implemented. Finally, the superiority of the ML approach is quantitatively demonstrated before a conclusion is drawn.

## II. EXPERIMENTAL SYSTEM OVERVIEW

### A. Chipless RFID Tag Design and Characterization

Four proof-of-concept chipless RFID topologies with two T-shaped resonant elements encoding all possible 2 bit combinations were inkjet-printed with silver nanoparticle on a polyethylene terephthalate substrate using a prototyping DMP2830 Dimatix inkjet printer. These topologies, shown in Fig. 1, form the basis for the set of measured data that will then be used to train the ML algorithm. Each vertical microstrip line introduces a different stopband resonance at approximately 3.45 and 5.7 GHz that can be used as IDs representing logic "00," "01," "10," and "11." The measured $S_{21}$ values of all four tags are shown in Fig. 2 and demonstrate the proper operation of the tags. The overall geometrical design for a T-shaped resonator is controlled by the key parameters summarized in Table I for each design of the resonator. Only the information of the transmission coefficients $S_{21}$, which serves as the channel transfer function between the
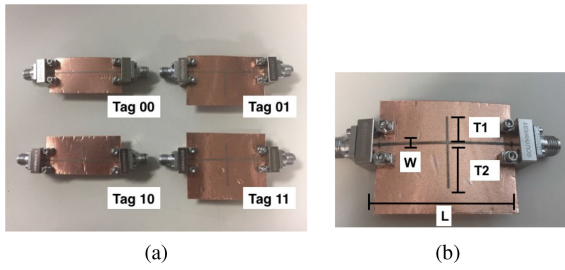
(a) (b)

Fig. 1. (a) Inkjet-printed chipless RFID tags. (b) Details showing the two T-shaped resonators encoding 2 bits.
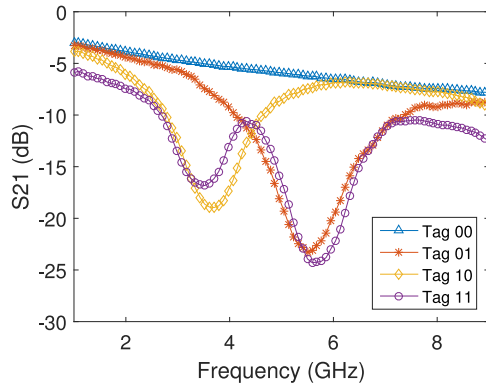


Fig. 2. Wire measurement $S_{21}$ results for the tags "00,""01," "10," and "11."

TABLE I
DESIGN PARAMETERS

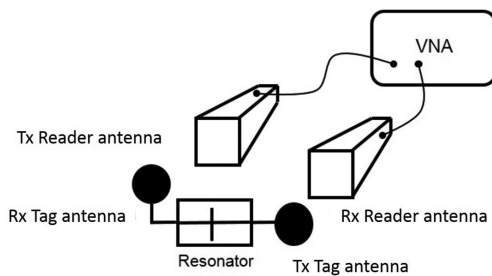| | Length(L) | Width(W) | Tline 1(T1) | Tline 2(T2) |
|---|---|---|---|---|
| Tag '00' | 40mm | 0.5mm | None | None |
| Tag '01' | 40mm | 0.5mm | None | 13mm |
| Tag '10' | 40mm | 0.5mm | 8mm | None |
| Tag '11' | 40mm | 0.5mm | 8mm | 13mm |



Fig. 3. Illustration of the measurement setup of the chipless RFID system.

reader antennas involves discrete frequencies, were of interest and used in the training.

### B. Measurements

The proposed chipless RFID system consists of the transmitter reader/tag antennas, receiver reader/tag antennas, and resonator tag attached to a styrofoam block, with a height of 10 cm from the ground, in a realistic environment, as shown in Fig. 3. The
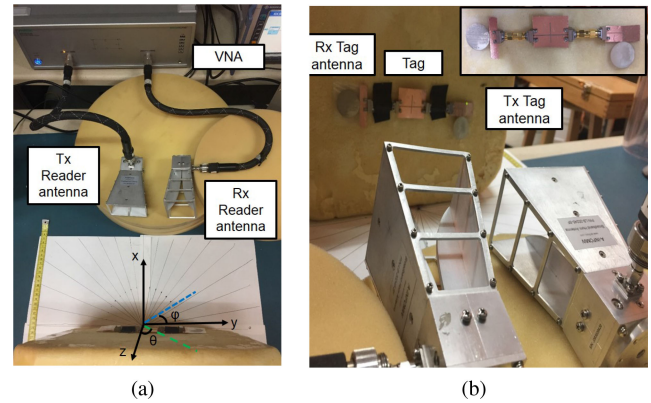


(a) (b)

Fig. 4. (a) Measurement setup. (b) Measurement setup from the reader side.

Tx and Rx antennas were cross-polarized to enhance crosstalk isolation and placed on the sponge, with the thickness of 4 cm. The *S*-parameters of the system were measured using a vector network analyzer, ZVA8 from Rohde&Schwarz, with a total of 816 measurements varying in the range of interrogation distances 5 up to 50 cm (in the step of 2 cm), in orientation (from $-40°$ to $+40°$ along $\phi$ angle, from $-40°$ to $+40°$ along $\theta$ angle) with consideration of the tag radiation pattern between the reader and tag antennas, as shown in Fig. 4, and in the presence of clutter in the space separating the tag and the reader antennas (80 cases out of the 816). To emulate the clutter, a paper box was used with the size of (28 cm × 25 cm × 5.6 cm) and was always placed in the middle of the distance between the tag and reader antennas. In other words, each tag underwent a total of 204 measurements varying the: 1) range of distances: 23; 2) orientation of angle: 160 from 5 to 50 cm in the step of 5 cm; and 3) presence of clutter: 21 from 10 cm (start from 10 cm taking the thickness of a paper box into account) to 50 cm in the step of 2 cm. Measured *S*-parameters from 1 to 10 GHz with 0.018 GHz interval in total 500 points per measurement were saved. The final size of the dataset (816 × 500) for training was determined based on different aspects such as training speed, complexity of classification, and so on.

### III. ML APPROACH

ML has been widely applied to numerous challenging problems to make predictions or perform pattern recognition. One method of learning called "supervised" learning is used to model a relationship between input features and desired output labels from a set of data (training dataset) [3]. The modeled relationship can be used to compute output labels for a set of new input features (test dataset) and typically done in the context of classification (when labels are from a set of discrete values) or regression (when labels are continuous). The "unsupervised" learning, in contrast, involves extracting the inherent structure of a dataset without reference to desired labels. Clustering of data points to discover hidden categories or classes from a dataset is a good example of an "unsupervised" learning method. Several studies on RFID-related applications have been done utilizing ML techniques; especially, the SVM classification has been
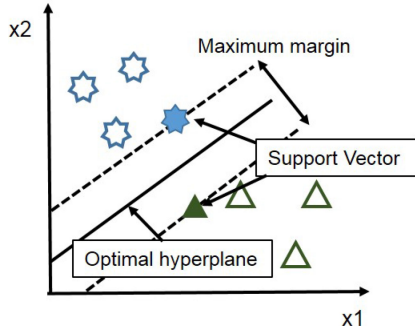
Fig. 5.　Basic concept of the SVM classification.



Fig. 6.　Proposed SVM tag ID detection.

TABLE II
COMPARISON ACCURACY OF THE DIFFERENT TRAINED MODELS

|  | Decision trees | Boosted trees | k-NN | SVM |
|---|---|---|---|---|
| Magnitude | 59.6 | 73.7 | 67.0 | 89.6 |
| Phase | 56.0 | 64.4 | 52.5 | 74.0 |
| Magnitude & Phase | 60.7 | 76.7 | 55.7 | 86.2 |
| Real | 58.1 | 68.7 | 56.1 | 94.4 |
| Imaginary | 61.9 | 75.8 | 60.7 | 93.2 |
| Real & Imaginary | 56.4 | 72.2 | 56.7 | **94.6** |
| Magnitude & Real | 55.2 | 76.8 | 62.6 | 92.5 |
| Magnitude & Imaginary | 59.0 | 64.6 | 60.9 | 92.3 |
| Magnitude & Real & Imaginary | 57.4 | 74.5 | 59.9 | 90.0 |

TABLE III
COMPARISON ACCURACY OF THE DIFFERENT KERNEL METHODS IN SVM

|  | Linear | Quadratic | Cubic | Gaussian |
|---|---|---|---|---|
| Kernel scale 1 | 94.6 | 93.1 | 92.9 | 26.0 |
| Kernel scale 3 | 99.1 | 93.3 | 90.2 | 39.9 |
| Kernel scale 5 | **99.3** | 93.9 | 87.1 | 51.0 |
| Kernel scale 7 | 99.0 | 94.2 | 90.6 | 62.0 |

used for personal healthcare application to collect and process multichannel data [4] and for learning-based self-localization to refine an estimation of the robot location [5]. By applying numerous RFID applications, ML techniques provide tremendous benefits in terms of the predicted RFID tag detectability and the learning-based localization.

## A. Classification: Support Vector Machine

In this application, we developed the SVM prediction model employing kernel tricks [6] with cross validation to evaluate the accuracy. This SVM techniques were chosen because they have been applied to various classification problems, such as development prediction models with high success [7]. The SVM essentially constructs a set of $(N - 1)$-dimensional hyperplanes in $N$-dimensional space to separate data points into groups used for classification, as shown in Fig. 5. When given a training dataset of $n$ points of the form $\vec{x}_n, y_n$, where $y_i$ are either 1 or $-1$ indicating the class to which the point $\vec{x}_i$ belongs, any hyperplane can be written as the set of points $\vec{x}$ satisfying $\vec{w} \cdot \vec{x} - b = 0$, where $\vec{w}$ is the normal vector to the hyperplane and the parameter $b/||\vec{w}||$ determines the offset of the hyperplane. In this respect, the optimal separating hyperplane for which the margin is maximum is essential to fall unseen test points far away from the hyperplane or in the margin. By employing a polynomial kernel function (1) of a hyperplane, the points $x$ in the $d$-dimensional feature space that are mapped into the hyperplane are defined by the relation, such as $\sum_i a_i k(x_i, x)$, making it easy to compute the similarity in the original space

$$k(x_i, x_j) = (\sigma(x_i^T \cdot x_j) + c)^d. \tag{1}$$

The linear kernel function, if $c = 0$ (and $d = 1$), was finally used here. The final decision function is given by the following equation for new predictions, which takes a dataset as input and gives a decision as output:

$$f(x) = \text{sign} \sum_i^n (a_i y_i) k(x_i, x_j) + b. \tag{2}$$

The SVM classifiers are trained on the entire training set using the optimized parameters and evaluated for their performances on the test sets with kernel scale ($\sigma$) 5, which is the free parameter invariant and independent of the input dimension, and it helps to avoid numerical difficulties during the calculation as the
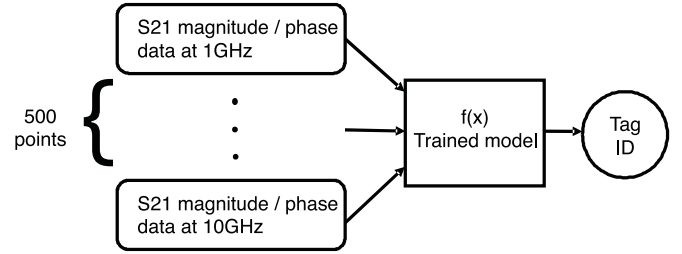
kernel values usually depend on the inner products of feature vectors, such as the polynomial kernel. Several types of the kernel functions with different kernel scales that were used in the training process are discussed in Section III-B. As mentioned in Section II-B, the measured $S_{21}$ parameters from 1 to 10 GHz with 0.018 GHz interval (in total 500 points per measurement) were used as input data for the training process, as shown in Fig. 6. The targeted output of the algorithm was set as the meaningful parameter in practical chipless RFID use contexts, namely, the IDs of the tags.

## B. Performance Evaluation

In order to detect the tag IDs, a training process using the proposed SVM classification with the measurement data previously described was implemented. The best SVM classifier achieved an accuracy of 99.3% when the combination of real and imaginary part information of the measured transmission coefficient $S_{21}$ was used for the training process. It should be stressed that the reported reading success rates are those obtained for raw data, without any crosstalk or environmental-clutter removal calibrations. The total dataset was divided into 80% of the dataset to train the model and 20% of the dataset to test the performance of the trained model using $k$-fold cross validation,

TABLE IV
CHIPLESS RFID TAG DETECTION TECHNIQUES IN THE FREQUENCY DOMAIN

| | Tag type | Detection Technique | Frequency (GHz) | Distance (cm) | Calibration | Anechoic chamber | Presence of object |
|---|---|---|---|---|---|---|---|
| [8] | Dual-band | Time-gating | 2.5-5 | 10-25 | background subtraction | Yes | No |
| [9] | Multi spiral | Amplitude & phase variation | 2-2.5 | 5-40 | use reference tag | Yes | No |
| [10] | Multi spiral | Signal space representation | 2-3.5 | up to 50 | windowed signal | Yes | No |
| [11] | Alphabetic | Frequency scanning, pattern recognition | 57-64 | 10-16 | background subtraction | Not clear | No |
| [12] | Dual L-type dipole | Short-time Fourier transform | 3-10 | 25 | None | Inside & outside | No |
| [13] | Concentric rectangular loop | Time-gating / free-space antenna response subtraction | 2-8 | up to 50 | None | No | No |
| **This work** | **T-shaped** | **SVM classification** | **0-10** | **5-50** | **None** | **No** | **Yes** |



Fig. 7. Confusion matrix for the SVM.



Fig. 8. Wire measured and time-gated signal for tag "10" at a distance of (a) 10 cm and (b) 30 cm.

which uses a limited sample in order to estimate how the model is expected to perform when used to make predictions on data not used during the training of the model resulting in a less biased or less optimistic estimation. In other words, 163 datasets were taken out from the total dataset that had not been used for the training to demonstrate the robustness of the chipless RFID measurement approach, especially in challenging contexts such as those used here with large antenna crosstalk, close-by clutter, and, thereby, difficult-to-extract tag IDs.

To identify the effect of the methods of different classifications known as decision trees, boosted trees, and $k$-NN with the SVM, each classification process was repeated and explored separately with different datasets composed of magnitude, phase, real part, imaginary part, and combined information of the measured transmission coefficient $S_{21}$. Table II shows the results that the accuracy from training increases up to 94.6% even for the measurements at longer ranges when we use the SVM method with the dataset composed of real and imaginary parts were combined. Also, several kernel functions were explored, including linear, quadratic, cubic, and Gaussian using different kernel scales $\sigma$. The obtained results show that a linear kernel method based on kernel scale 5 outperforms the other methods for detecting tag's IDs with an accuracy of 99.3%, as shown in Table III. In this context, the algorithm demonstrates a remarkable performance for detecting tag's IDs. The confusion matrix using the combination of real and imaginary data for SVM with kernel scale 5, known as an error matrix in the field of ML classification, is shown in Fig. 7 that allows more detailed analysis and visualization of the performance of the trained model with the SVM. It can be easily seen that the overall classification is 99.3% and above 99% for all different tag IDs.

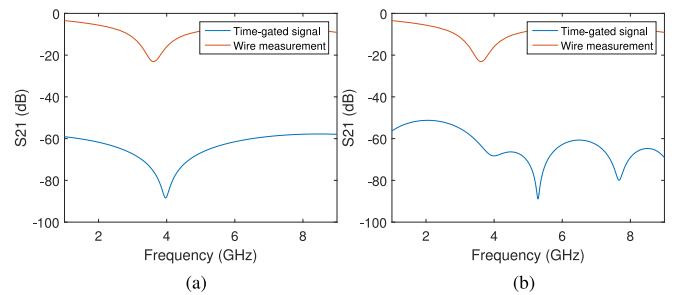One can use different detection techniques [8]–[13] to identify chipless RFID tag-ID-based frequency-domain information, as reviewed in Table IV. To verify the fabricated chipless RFID tag IDs and show the limitations of existing techniques, the standard chipless RFID tag detection technique known as time gating was used: Its results are shown in Fig. 8, for distances of 10 and 30 cm. The process of time gating follows the steps proposed in [8]. The frequency response of the tag "10" at a tag–reader distance of 10 cm—with a 3–4 ns time window—was readily obtained. However, at a distance of 30 cm, the technique was unable to reliably detect the tags, as shown with the example of ID "10" in Fig. 8(b), compared to the wire measurement $S_{21}$ result for the tag "10," By contrast, our SVM-based technique achieved better than 98% read rates at that distance, without requiring the knowledge of the distance and, therefore, the time-gating delay. This letter reveals the remarkable read/interrogate enhancement that can be achieved with this technique, without any required knowledge of the environment, and in practical conditions varying by operating distance, orientation, and in dynamic cluttered environments without the need for additional calibration.

## IV. CONCLUSION

In this letter, the implementation of a specific ML technique, SVM classification, to detect the chipless RFID tag IDs was demonstrated. In addition, high reading accuracies (above 98%) were achieved without environmental calibration, even in the cases of different orientations and with the presence of objects between the reader and tag antennas. The proposed detection model is very scalable and generalizable to context for a large number of tags, with a much higher number than 2 bits used here, and with additional influence factors. The work reported here relies on a specific method but opens the door for a broad area of research that could greatly enhance the state-of-the-art of chipless RFID detection algorithms and techniques.

## REFERENCES

[1] K. Finkenzeller, *RFID Handbook: Fundamentals and Applications in Contactless Smart Cards and Identification*. Hoboken, NJ, USA: Wiley, 2003. [Online]. Available: https://books.google.com/books?id=KQLqjwEACAAJ

[2] S. Preradovic, I. Balbin, N. C. Karmakar, and G. Swiegers, "A novel chipless RFID system based on planar multiresonators for barcode replacement," in *Proc. IEEE Int. Conf. RFID*, Las Vegas, NV, USA, Apr. 2008, pp. 289–296.

[3] M. A. Hearst, S. T. Dumais, E. Osuna, J. Platt, and B. Scholkopf, "Support vector machines," *IEEE Intell. Syst. Appl.*, vol. 13, no. 4, pp. 18–28, Jul. 1998.

[4] S. Amendola, R. Lodato, S. Manzari, C. Occhiuzzi, and G. Marrocco, "RFID technology for IoT-based personal healthcare in smart spaces," *IEEE Internet Things J.*, vol. 1, no. 2, pp. 144–152, Apr. 2014.

[5] K. Yamano, K. Tanaka, M. Hirayama, E. Kondo, Y. Kimuro, and M. Matsumoto, "Self-localization of mobile robots with RFID system by using support vector machine," in *Proc. IEEE/RSJ Int. Conf. Intell. Robots Syst.*, vol. 4, Sep. 2004, pp. 3756–376.

[6] T. Hofmann, B. Schölkopf, and A. J. Smola, "Kernel methods in machine learning," *Ann. Statist.*, vol. 36, no. 3, pp. 1171–1220, 2008.

[7] V. N. Vapnik, *Statistical Learning Theory*. New York, NY, USA: Wiley-Interscience, 1998.

[8] D. Girbau, J. Lorenzo, A. Lazaro, C. Ferrater, and R. Villarino, "Frequency-coded chipless RFID tag based on dual-band resonators," *IEEE Antennas Wireless Propag. Lett.*, vol. 11, pp. 126–128, 2012.

[9] S. Preradovic, I. Balbin, N. C. Karmakar, and G. F. Swiegers, "Multiresonator-based chipless RFID system for low-cost item tracking," *IEEE Trans. Microw. Theory Techn.*, vol. 57, no. 5, pp. 1411–1419, May 2009.

[10] P. Kalansuriya, N. C. Karmakar, and E. Viterbo, "On the detection of chipless RFID through signal space representation," *Ann. Telecommun.*, vol. 68, no. 7, pp. 437–445, Aug. 2013.

[11] L. M. Arjomandi and N. C. Karmakar, "An enhanced chipless RFID system in 60 GHz using pattern recognition techniques," in *Proc. 48th Eur. Microw. Conf.*, Madrid, Spain, Sep. 2018, pp. 973–976.

[12] A. Ramos, E. Perret, O. Rance, S. Tedjini, A. Lázaro, and D. Girbau, "Temporal separation detection for chipless depolarizing frequency-coded RFID," *IEEE Trans. Microw. Theory Techn.*, vol. 64, no. 7, pp. 2326–2337, Jul. 2016.

[13] F. Costa, S. Genovesi, and A. Monorchio, "Normalization-free chipless RFIDs by using dual-polarized interrogation," *IEEE Trans. Microw. Theory Techn.*, vol. 64, no. 1, pp. 310–318, Jan. 2016.